

COUPLED-DOMAIN MODELLING OF ELECTROSTATIC ENERGY SCAVENGERS AND POWER MANAGEMENT CIRCUITRY

D. Hohlfeld¹, B. Op het Veld², R. J. M. Vullers¹, J de Boeck¹

¹Holst Centre / IMEC-NL, Eindhoven, The Netherlands; ²Philips Research, Eindhoven, The Netherlands

Abstract: In this work a new approach for modelling electrostatic energy scavengers and their related circuitry is presented. For the first time a coupled-domain electromechanical scavenger model is derived from the underlying physics and implemented in a behavioural simulator. The model is coupled to a harvesting and voltage conversion circuitry. We apply the model to electrostatic scavengers which are based on a gap-closing MEMS capacitor. Optimum resistive load and electrical in- / output power have been determined.

Key Words: coupled domain simulation, electrostatic energy scavenging

1. INTRODUCTION

Up to now piezoelectric and electrostatic vibrational scavengers have been modelled analytically through lumped element models which employ equivalent electrical circuits [1]-[2] for description of dynamic behaviour. Electrical components such as resistors, inductors and capacitors are used to describe the effects of damping, mass inertia and spring stiffness. A transformer translates mechanical parameters like force and velocity into their electrical equivalents, voltage and current. These conventional models can be solved through established circuit analysis techniques.

The proposed modelling approach advances the model by inclusion of non-linear damping effects, switches and variable capacitors. Finally the mutual interaction between the mechanical and electrical domain is implemented, while the work in [3] is based on the electrical domain only. As the model is based on a behavioural description it enables the design of an optimized power management circuitry in a single simulation environment.

Advanced microelectromechanical structures have recently been treated by the use of electrical circuit representation [4]. The implementation of variable elements like MEMS-capacitors could only be indirectly achieved. The use of non-linear elements, which depend on time or state variables (e.g. position and electrical charge), is not feasible with conventional circuit simulators like SPICE.

2. DEVICE DESCRIPTION

The working principle of the scavenger, as described in [3], is based on a variable MEMS-capacitor. Its capacitance varies due to resonant excitation of a seismic mass. Charge, taken from a voltage source, is transferred via a variable capacitor to a storage capacitor; thus charging it to higher potentials. This is achieved by utilizing mechanical energy to separate the electrodes of a parallel plate capacitor against the counteracting electrostatic forces.

The gained energy raises the potential of the charge isolated on the variable capacitor. In this way the structure acts as a mechanical equivalent to an electrical charge pump.

3. DEVICE MODELLING

The present work uses the non-linear differential equations for describing the mechanical dynamics of the energy scavenger (see Figure 1) and its electrical circuit (see Figure 2).

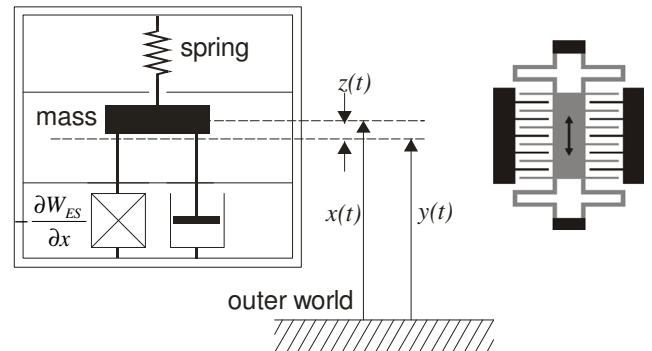


Figure 1: (left) Lumped mechanical model of the resonant scavenger including non-linear electrostatic and viscous damping. (right) schematic representation of a gap-closing electrostatic scavenger.

A mass is suspended to a frame via a spring. During motion linear and non-linear damping forces are present. The mass dynamics are described by the following equation:

$$m \ddot{z} + F_{ES} + d \dot{z} + k z = -m \ddot{y} \quad \text{with } z = x - y \quad (1)$$

Here, F_{ES} and $d \dot{z}$ are the electrostatic and mechanical damping forces which act on the mass. The variables x and y denote the mass and frame displacements respectively. The electrostatic damping force can be derived from the energy stored in the capacitor.

$$F_{ES} = -\frac{\partial W_{ES}}{\partial x} = \frac{1}{2} \frac{Q^2}{\epsilon A} \frac{z}{d} \quad (2)$$

As the charge is kept constant during motion, the damping force depends linearly on the displacement. Equation (2) couples the mechanical domain with the electrical circuit representation (described below) as F_{ES} is determined by the present charge.

The variable capacitor is a key element in the harvesting circuit as shown Figure 2. Two switches (S_1 and S_2) control the (dis-)charging of the MEMS capacitor.

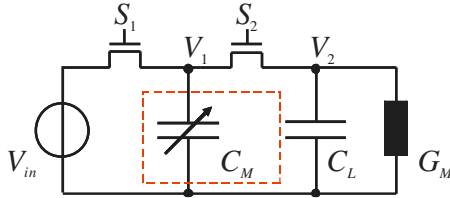


Figure 2: Electrical harvesting circuit for a variable capacitor (diodes may be used as passive switches).

We can compose the following system of differential equations from Kirchhoff's Current Law for the potentials in nodes V_1 and V_2 .

$$\begin{bmatrix} C_M & 0 \\ 0 & C_L \end{bmatrix} \dot{v} + \underbrace{\begin{bmatrix} G_1 + G_2 + \dot{C}_M & -G_2 \\ -G_2 & G_2 + G_L \end{bmatrix}}_K v = \begin{bmatrix} V_{in} G_1 \\ 0 \end{bmatrix} \quad (3)$$

As the system matrices are time-dependent (due to the varying capacitance C_M) a straightforward analytical solution is not possible here. However, an implicit presentation for \dot{v}_1 and \dot{v}_2 can be given by

$$\dot{v}_1 = \frac{1}{\det K} \det \begin{bmatrix} V_{in} G_1 - C_M \dot{v}_1 & -G_2 \\ -C_L \dot{v}_2 & G_2 + G_L \end{bmatrix} \quad (4)$$

$$\dot{v}_2 = \frac{1}{\det K} \det \begin{bmatrix} G_1 + G_2 + \dot{C}_M & V_{in} G_1 - C_M \dot{v}_1 \\ -G_2 & -C_L \dot{v}_2 \end{bmatrix} \quad (5)$$

The variable capacitance of an antisymmetric gap-closing capacitor, as shown in Figure 2 is

$$C_M = C_0 \left(1 - (z/d)^2\right)^{-1} \quad \text{with } C_0 = 2N \cdot \epsilon h l / d \quad (6)$$

In equation (6) the parameters ϵ , z , d , N , h and l are the permittivity, displacement, initial gap, number of comb fingers, finger height and length respectively. If we can assume harmonic motion for the mass (e.g. $z = Z_0 \sin(\omega t)$) one can solve numerically for v_1 and v_2 . We will see that Z_0 rather depends on v_1 which makes a coupled solution of the mechanical and electrical domain mandatory.

4. MODELLING RESULTS

Initially we solve the mechanical and electrical domain independently in order to show the significance of coupled simulation. Compared to

previous work [3] exact description of damping due to an electrostatic force is included in the mechanical model.

We will load the energy scavenger with a matched resistive load and connect a voltage conversion circuit for coupled-domain simulation.

4.1. Mechanical simulation

Equation (1) may be solved analytically if only linear damping is present under harmonic excitation (see Figure 3).

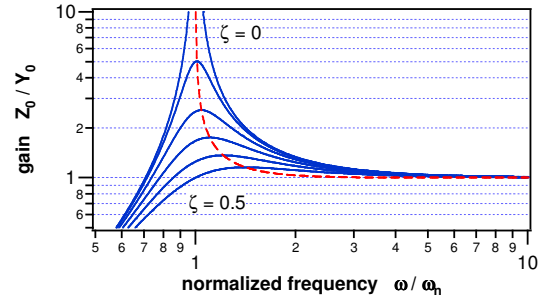


Figure 3: Gain curves for a resonator with linear damping (normalized damping coefficient $\zeta = d/2m\omega_n$).

A transient solution of equation (1) near the resonators resonance frequency results in harmonic motion of the mass. The amplitude is settling at the value defined through the corresponding gain (Figure 4).

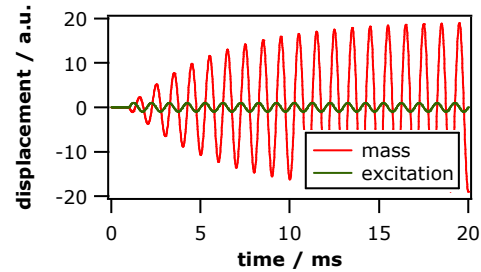


Figure 4: Motion of the suspended seismic mass under the influence of viscous damping.

If noise excitation is applied, the resonator acts as a mechanical filter. According to its bandwidth it selects a certain part of the input spectrum and responds with an amplified displacement (Figure 5).

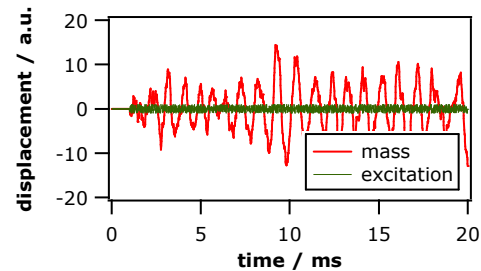


Figure 5: Resultant motion of the mass under broadband excitation (bandwidth limited white noise spectrum).

4.2. Electrical modelling

For purely electrical analysis we assume harmonic motion of the mass which results in a capacitance change according to equation (6).

Using equations (4-5) we numerically solve for the potential v_1 and v_2 . If both capacitors are completely discharged at $t=0$ one obtains the data shown in Figure 6.

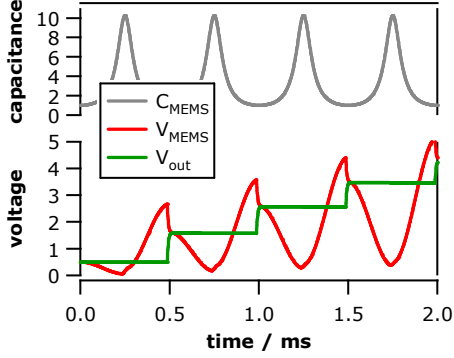


Figure 6: Capacitance change and voltage of the circuit shown in Figure 2. The incremental charge transfer increases the output voltage gradually.

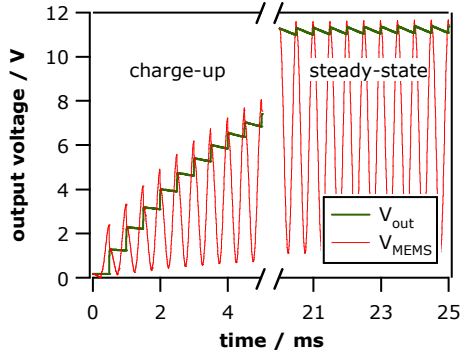


Figure 7: Saturation of output with an input voltage of 1 V.

With $\tau = C_L/G_L$ the output voltage and average output power are:

$$V_{out}(t) = V_{in} C_{max} / [C_{min} + C_L(1 - e^{-t_d/\tau})] e^{-t/\tau} \quad (7)$$

$$P_{out} = \frac{1}{T} \int_0^T V_{out}^2(t) G_L dt = \frac{1}{2} V_{out,max}^2 G_L \frac{\tau}{t_d} (1 - e^{-2t_d/\tau}) \quad (8)$$

We finally implemented a DC/DC converter with the harvesting circuit to store the converted electrical

energy in an energy storage system (ESS) like a Li-ion battery or super capacitor. For both ESSs, the DC/DC converter should convert from a high voltage ($> 10V$) down to a rather low voltage. The voltage range of a Li-ion battery is 3.0-4.2 V and a super capacitor uses 2.5-2.7 V. This means that a capacitive or inductive down-converter is used. The advantage of an inductive DC/DC converter is the rather big efficiency over a wide input voltage range where the capacitive DC/DC converter needs to switch to a different conversion ratio. However, the disadvantage is the usage of an inductor with a large value where the capacitive DC/DC converter can be integrated completely.

4.3. Electro-mechanical modelling

We now couple the mechanical and electrical models with a transducer element. This is done using a two port element which has two position values and two potentials as parameters. The state variable is the capacitor's charge. From the difference of the position values the capacitance is determined according to equation (6). The acting force is calculated using equation (2). The current through the electrical ports is then defined by $i_c = C_M \dot{v}_1$. The behavioural model, as implemented in Saber®, is shown in simplified form in Figure 6.

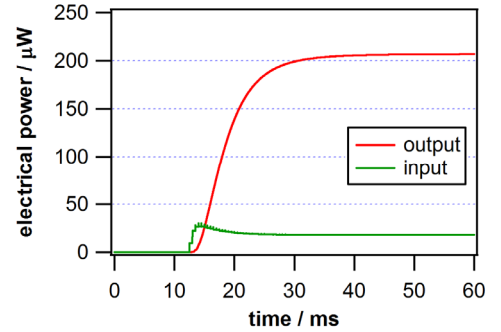


Figure 9: Initial phase of the energy scavenging process. Initially electrical power has to be drawn from the voltage source for repeatedly charging the variable capacitor.

We performed transient simulations of the model shown in Figure 8. The variable capacitor is incrementally charged by the voltage source, thereby consuming electrical power. This initial process is illustrated in Figure 9.

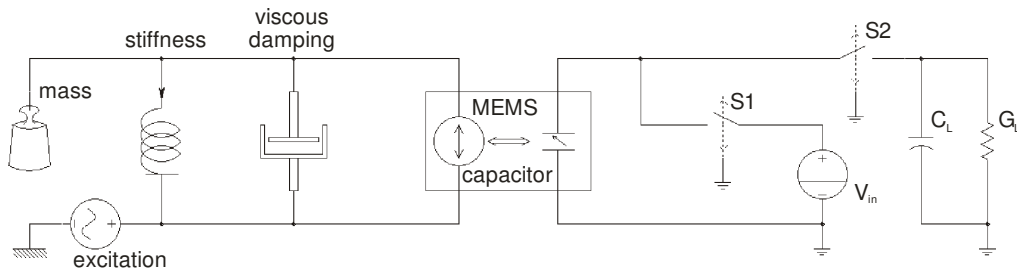


Figure 8: Simplified behavioral model for the energy scavenger. An electro-mechanical model of the variable capacitor couples the mechanical domain (left) with the harvesting circuitry (right). The logic for controlling the switches is not shown.

After equilibrium between dissipated and gained power has been reached, a less electrical power is drawn from the voltage source. Still, this contribution has to be considered in order to give correct electrical power output values. Repeated transient analyses were performed to obtain the data shown in Figure 10.

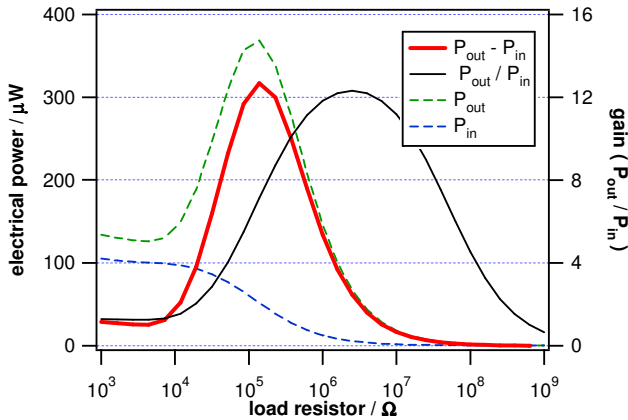


Figure 10: Matching the energy scavenger with a resistive load. In the present case maximum power is obtained for a load of 140 kΩ. Optimum utilization of the provided electrical power occurs at 2.5 MΩ.

We further propose a strategy how to optimize the parameters of the scavenger system.

Load resistor: In order to maximize the electrical output power the load resistor was varied and transient analyses were performed. The results for varying load resistance are shown in Figure 10. The gained electrical power is shown versus the load resistance. It is peculiar that most efficient use of the provided electrical power occurs for a higher load resistance.

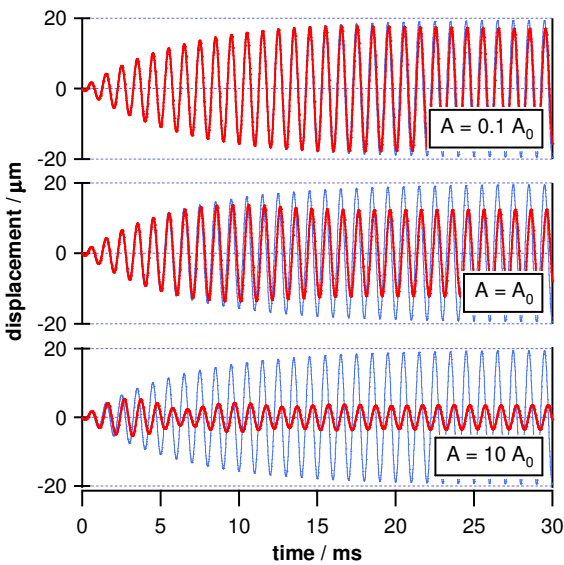


Figure 11: Effect of electrostatic damping on the amplitude. In contrast to purely mechanically damped motion (blue) the biasing voltage ($V_{in} = 1$ V) may strongly damp the motion of the mass (red) depending on the capacitor area A .

Impact of capacitor area: Changing the capacitance C_0 (capacitance at centre position $z = 0$) shows two effects. A high value is required for efficiently charging the load capacitor with few cycles. However, the generated electrostatic forces, which damp the mass' motion, might be too high to allow full displacement. This prevents the mass from reaching its designated amplitude (Figure 11).

Charging period: After optimizing the load resistor the most effective way of further increasing the output power is to modify the period in which the variable capacitor is charged. In the optimum case the period in which S_1 is closed (thus charging C_M) should be no longer than 3τ (τ being the time constant for charging C_M) and S_1 should be opened instantly as C_M achieves its maximum value (carrying maximum charge).

5. CONCLUSIONS

It was shown that independent mechanical and electrical modelling is insufficient for correct description of the system's dynamics. The inclusion of electrostatic damping forces has proven to advance the scavenger description to valuable electro-mechanical model. It was also stated that the input voltage source provide small, but not negligible, amount of electrical power. The impact of various parameters on the output power was discussed and the load resistance and charging period were identified as of outermost importance.

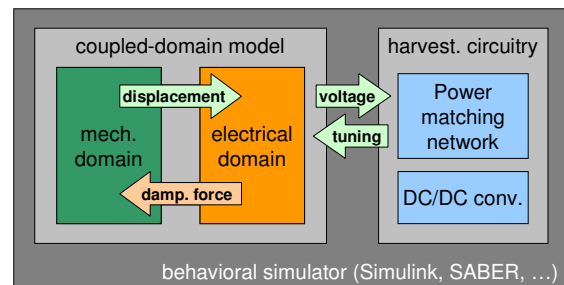


Figure 12: Interaction of the coupled-domain scavenger model and accompanying harvesting circuitry within a single design environment

It is further envisaged to couple the electro-mechanical model with electrical control mechanisms to influence the systems dynamics.

REFERENCES

- [1] Poulin, G., et al., *Sensors and Actuators A-Physical*, **116**, pp. 461-471, 2004.
- [2] Mitcheson, P. D., et al., *J. Microelectrom. Systems*, **13**, pp. 429-440, 2004.
- [3] Chiu, Y., et al., *Microsystem Technologies*, **13**, pp. 1663-1669, 2007.
- [4] Zhu, Y., et al., *Journal of Micromechanics and Microengineering*, **17**, pp. 1059-1065, 2007